CLM-P748

CLM-P748

UKAEA

Preprint

TEST-PARTICLE TRANSPORT DUE TO FLUCTUATING MAGNETIC FIELDS IN TOKAMAKS

A. THYAGARAJA
I. L. ROBERTSON
F. A. HAAS

CULHAM LABORATORY
Abingdon Oxfordshire

1985

CLM-P 748

TEST-PARTICLE TRANSPORT DUE TO FLUCTUATING MAGNETIC FIELDS IN TOKAMAKS

A. Thyagaraja, I.L. Robertson and F.A. Haas

UKAEA Culham Laboratory, Abingdon, Oxon., UK

(Euratom/UKAEA Fusion Association)

Abstract

The transport of charged test-particles in the presence of given magnetic fluctuations and collisions is investigated from two approaches, namely, the Langevin and corresponding Fokker-Planck equations. Analytic discussion of the Fokker-Planck equation shows the radial particle and energy fluxes to be purely diffusive. The Langevin approach confirms the validity of the Fokker-Planck perturbative calculation for sufficiently small fluctuation amplitudes. From the Fokker-Planck theory we derive an effective parallel thermal diffusivity valid for all collisionalities, and show that the high collisionality result of Braginskii and the low collisionality form previously conjectured by the authors, are recovered. Application of the theory to TFR leads to qualitative agreement with the published observations.

(Submitted for publication in Plasma Physics and Controlled Fusion)

April 1985

1. INTRODUCTION

In this paper we investigate analytically and numerically the transport of charged test-particles in the presence of magnetic fluctuations, taking account of collisions. We set up and solve the Langevin equations for the test-particles, and also the corresponding Fokker-Planck equation. For simplicity we restrict ourselves to a periodic cylinder geometry with prescribed mean and fluctuating fields. We neglect the Larmor motions of the test-particles about the field lines and any drifts; thus, in this model, the instantaneous velocity of a test-particle is always parallel to the instantaneous field direction. The effect of collisions is represented by a random Langevin force and a prescribed collision time τ. At each collision a test-particle is allowed to move in a random direction by a fixed step-length ρ. In the absence of field fluctuations the Brownian motion of the test-particle results in a radial diffusivity, $D_{\perp o} = \rho^2/4\tau$. The purpose of the present investigation is to examine the conditions and extent to which this "background" transport is modified by the presence of magnetic fluctuations.

We find that for fluctuation amplitudes typical of tokamaks the Fokker-Planck and Langevin approaches lead to essentially the same confinement times. It is found that even single coherent fluctuations (fixed frequency, ω, m, n) can under suitable conditions result in significant test-particle transport. Furthermore, the radial transport due to a given mode has a resonant behaviour with respect to the collisionality parameters $\omega\tau$ and $\frac{v_{the}\tau}{qR}$ in the sense that the confinement time has a minimum when these parameters are of order unity. The Fokker-Planck calculations in particular show several interesting features. Firstly, both radial energy and particle fluxes are purely diffusive and contain density and temperature gradient terms. Secondly, the particle and thermal diffusivities differ only by a numerical form factor and are generally of the same order. Thirdly, the Fokker-Planck theory gives parallel transport coefficents for arbitrary collisionality. These are shown to reduce to the Braginskii form at high collisionality and to previously conjectured forms at low collisionality (THYAGARAJA et

al., 1980). Calculations with an ensemble of time-dependent magnetic fluctuations show that for conditions typical of TFR, the test-particle transport model captures many features of the observed electron anomalous transport.

The paper concludes with a brief discussion of the relationship between test-particle transport and actual plasma transport, as well as a comparison with earlier magnetic turbulence theories.

2. ANALYTIC FORMULATION

(a) Langevin Approach

We begin with the Langevin formulation. Taking the usual r, θ, z coordinates, we consider a cylindrical model of a tokamak equilibrium. The minor radius is denoted by a and the periodicity length is $2\pi R$; the longitudinal field B_z is taken to be constant and the mean poloidal field B_θ is a function of radius, r, only. We further assume a prescribed fluctuating field $\underline{\delta B}$ (r, θ, z, t) to be superimposed upon this equilibrium. We consider the motion of a test-particle in the resulting magnetic field to be governed by

$$\frac{d\underline{r}}{dt} = v_{\parallel} \frac{\underline{B}\,(\underline{r},\, t)}{B} , \tag{1}$$

where $v_{\parallel}$ is a random variable determined by the equation

$$\frac{dv_{\parallel}}{dt} + \frac{v_{\parallel}}{\tau} = R(t) \; ; \tag{2}$$

see, for example, UHLENBECK and ORNSTEIN (1930).

To avoid misunderstanding it should be noted that the above equations refer to a frame of reference in which the plasma ions are at rest. The plasma electrons will in general have a drift relative to the ions which is however negligible compared to their thermal velocity. We have likewise assumed that the test-electrons have negligible drift velocities as compared with their thermal velocity v_{the}, which is taken to be the same as the plasma electrons. Although we consider time

dependent fields in Eq. (1), the acceleration of the test-electrons due to the associated parallel electric field is neglected in Eq. (2) in comparison with the random Langevin forces. The validity of these assumptions with respect to tokamak applications is discussed later.

The parameter τ represents a 90° collision time, while R(t) is a random function such that for $t >> \tau$, then $\langle v_{\parallel} \rangle = 0$ and $\langle v_{\parallel}^2 \rangle = v_{the}^2$. For simplicity we take the parameters v_{the}^2 and τ to have uniform and constant values typical of tokamaks. Given the form of R(t) and a specified number of particles, Eqs. (1) and (2) have been solved numerically by the Monte Carlo method. These equations are evolved for a time τ, at which instant the position of the particles are displaced in a random direction through a fixed distance ρ ; the latter parameter is also prescribed. This procedure is repeated throughout the calculation and the long-term evolution of the spatial density of particles is obtained. It should be noted that in this model, stochasticity enters explicitly through: (a) the initial conditions, (b) the function R(t), and (c) the random direction of the displacement ρ at each "collision". The magnetic fields themselves are prescribed, deterministic functions of position and t .

The above formulation based on the two Langevin equations for $v_{\parallel}$ and $\underline{r}$, enables us in principle to discuss the evolution of the distribution function $f(\underline{r}, v_{\parallel}, t)$ in complete detail. We consider the steady-state or "source" problem. In this, the total number of particles is kept constant throughout the calculation. To accomplish this, as test-particles cross the surface $r = a$, they are reinjected into the solution domain according to a suitably prescribed source distribution. Starting from an arbitrary initial distribution, the system will settle to an essentially steady-state after some characteristic confinement time, τ_{conf}; other parameters being fixed, the final steady-state is determined uniquely by the source distribution. The rate of recycling particles is an outcome of the calculation and is a measure of the confinement properties of the system. These points are further explained and applied in section 3 and an appendix.

(b) Fokker-Planck Approach

We now turn to the complementary Fokker-Planck formulation. Standard arguments from Brownian motion theory (VAN KAMPEN, 1983) imply that the test-particle distribution function $f(\underline{r}, v_\parallel, t)$ corresponding to the Eqs. (1) & (2) satisfies the Fokker-Planck equation

$$\frac{\partial f}{\partial t} + v_\parallel \nabla\cdot(\underline{b}f) = \frac{1}{\tau}\frac{\partial}{\partial v_\parallel}\left(v_{the}^2 \frac{\partial f}{\partial v_\parallel} + v_\parallel f\right) + \frac{\rho^2}{4\tau}\nabla^2 f + S(v_\parallel, \underline{r}) , \qquad (3)$$

where $\underline{b} = \frac{\underline{B}}{B}$ and S represents the particle source. The relationship between Eq. (3) and the Fokker-Planck equation satisfied by the plasma electrons will be discussed in Section 5. We shall develop the solution of Eq. (3) in terms of the small parameters $\delta B_r/B_o$. As a consequence of our analysis it will turn out that for τ typical of tokamaks the parameter τ/τ_{conf} (where the confinement time τ_{conf} is defined later) is also very small. Note that in the following we assume $\omega \neq 0$ but otherwise <u>arbitrary</u>. In particular the parameters $\omega\tau$ and $v_{the}\tau/qR$ can take any values. In the present work we write

$$\underline{b} = \underline{b}_o(r) + \underline{\delta b}(\underline{r}, t) \qquad (4)$$

where $\left|\delta b\right| << 1$. The perturbation $\underline{\delta b}$ is again a specified function of position and time, and periodic in θ, z and t. We seek solutions of Eq. (3) in the form

$$f = f_o(r, v_\parallel) + \delta f(\underline{r}, v_\parallel, t) . \qquad (5)$$

Assuming non-zero frequencies, it is feasible to solve Eq. (3) perturbatively in the limit $\rho \to 0$. Following Eq. (5) we make the following ansatz for f_o :

$$f_o(r, v_\parallel) = \frac{n_o(r)}{\sqrt{2\pi}} \frac{1}{v_{the}(r)} e^{-\frac{v_\parallel^2}{2v_{the}^2(r)}} + g(r, v_\parallel) \qquad (6)$$

The functions $n_o(r)$, $v_{the}(r)$ and g are to be determined. We assume g to be much smaller than the first, Maxwellian term. Averaging Eq. (3) over t, θ, z, we find that f_o must satisfy

$$\frac{1}{\tau}\frac{\partial}{\partial v_\parallel}\left(v_{the}^2\frac{\partial f_o}{\partial v_\parallel} + v_\parallel f_o\right) = \frac{v_\parallel}{r}\frac{\partial}{\partial r}\left(r\langle\delta b_r \delta f\rangle\right) - \langle S(v_\parallel, \underline{r})\rangle \ . \qquad (7)$$

The dominant term is the one involving the collision time τ. The leading order solution is given by the first term in Eq. (6), where $n_o(r)$ and $v_{the}(r)$ are as yet arbitrary. Substituting (6) into (7) we find that g must satisfy

$$\frac{1}{\tau}\frac{\partial}{\partial v_\parallel}\left(v_{the}^2\frac{\partial g}{\partial v_\parallel} + v_\parallel g\right) = v_\parallel\frac{1}{r}\frac{\partial}{\partial r}\left(r\langle\delta b_r \delta f\rangle\right) - \langle S(v_\parallel, \underline{r})\rangle \ . \qquad (8)$$

In order to solve Eq. (8) and obtain a unique solution, we impose the subsidiary conditions,

$$\int_{-\infty}^{\infty} g\ dv_\parallel = \int_{-\infty}^{\infty} v_\parallel^2\ g\ dv_\parallel = 0 \ . \qquad (9)$$

These imply that $n_o(r)$ and $v_{the}(r)$ are the physical test-particle number density and thermal velocity, in the leading order, respectively.

Multiplying Eq. (8) by 1 and $\frac{1}{2}m_e v_\parallel^2$ we find the integrability conditions,

$$\frac{1}{r}\frac{\partial}{\partial r}\left(r\langle\delta b_r \int_{-\infty}^{\infty} v_\parallel\ \delta f\ dv_\parallel\rangle\right) = \langle\int_{-\infty}^{\infty} S(v_\parallel, \underline{r})\ dv_\parallel\rangle \ . \qquad (10)$$

$$\frac{1}{r}\frac{\partial}{\partial r}\left(r\langle\delta b_r \int_{-\infty}^{\infty}\frac{1}{2}m_e v_\parallel^3\ \delta f\ dv_\parallel\rangle\right) = \langle\int_{-\infty}^{\infty}\frac{1}{2}m_e v_\parallel^2\ S(v_\parallel, \underline{r})\ dv_\parallel\rangle \ . \qquad (11)$$

It will turn out that Eqs. (10) and (11) are the 'transport' equations

satisfied by $n_o(r)$ and $v_{the}^2(r) \equiv \frac{T_{oe}}{m_e}$ for the given particle source $\langle \int_{-\infty}^{\infty} S(v_\parallel, \underline{r})\, dv_\parallel \rangle$ and energy source $\langle \int_{-\infty}^{\infty} \frac{1}{2} m_e v_\parallel^2\, S(v_\parallel, \underline{r})\, dv_\parallel \rangle$. It will be seen that the smallness parameter implicit in the ansatz Eq. (7) is τ/τ_{conf} , where τ_{conf} is the characteristic confinement time. Linearising Eq. (3) with respect to small amplitudes and neglecting g , we obtain the linear (in δf) equation,

$$\frac{\partial}{\partial t}\ \delta f + v_\parallel\, \underline{b}_o(r)\cdot\nabla\delta f + \delta b_r\, v_\parallel \frac{\partial}{\partial r} \left\{ \frac{n_o}{\sqrt{2\pi}} \frac{1}{v_{the}} e^{-\frac{v_\parallel^2}{2v_{the}^2}} \right\}$$

$$= \frac{1}{\tau} \frac{\partial}{\partial v_\parallel} \left(v_{the}^2 \frac{\partial \delta f}{\partial v_\parallel} + v_\parallel \delta f \right) . \qquad (12)$$

In deriving Eq. (12) we have made use of $\nabla\cdot\underline{\delta B} = 0$ and the tokamak ordering $B_o(r) \simeq B_{oz}$ (uniform). This linear inhomogeneous equation for δf is solved by Fourier analysis in terms of the given δb_r and the as yet undetermined $n_o(r)$ and $T_{oe}(r)$. The solution when substituted in Eq. (10) and (11) yields equations for $n_o(r)$ and $T_{oe}(r)$. Solution of Eq. (8) for g can be used to obtain the parallel current in terms of the momentum source $\langle \int_{-\infty}^{\infty} v_\parallel\, S(v_\parallel, \underline{r})\, dv_\parallel \rangle$.

Before solving the problem in detail it is instructive to exhibit the dependence of the particle and energy fluxes on n_o, $\frac{dn_o}{dr}$, T_{oe} , $\frac{dT_{oe}}{dr}$ and the fluctuation spectrum. To see this, we assume

$$\delta b_r = \int_{-\infty}^{\infty} d\omega \sum_{m,n} \bar{b}_{mn}(r, \omega)\, e^{i\left(m\theta + \frac{nz}{R} + \omega t\right)} \qquad (13)$$

$$\delta f = \int_{-\infty}^{\infty} d\omega \sum_{m,n} \bar{F}_{mn}(r, \omega, v_{\parallel})\, e^{i\left(m\theta + \frac{nz}{R} + \omega t\right)} \qquad (14)$$

Substituting in Eq. (12) and introducing the transformation

$v_{\parallel} = v_{the}(r)x$, and defining the functions $\bar{W}(x, r)$ and $\bar{Z}(x, r)$ [where the dependence on the mode numbers is implied] through,

$$\bar{F}_{mn} = \frac{\bar{W}(x,r)}{\sqrt{2\pi}}\, \tau\, \delta b_r \frac{dn_o}{dr} e^{-\frac{x^2}{4}} + \frac{\bar{Z}(x,r)}{\sqrt{2\pi}}\, \tau \delta b_r\, n_o \frac{1}{v_{the}} \frac{d\, v_{the}}{dr} e^{-\frac{x^2}{4}} , \qquad (15)$$

we obtain the equations

$$\frac{d^2\bar{W}}{dx^2} + \bar{W}\left\{\frac{1}{2} - \frac{x^2}{4} - i\tau\left(\omega + x\, v_{the}\, k_{\parallel}\right)\right\} = x\, e^{-\frac{x^2}{4}} \qquad (16)$$

$$\frac{d^2\bar{Z}}{dx^2} + \bar{Z}\left\{\frac{1}{2} - \frac{x^2}{4} - i\tau\left(\omega + x\, v_{the}\, k_{\parallel}\right)\right\} = (x^3 - x)\, e^{-\frac{x^2}{4}} . \qquad (17)$$

The test-particle flux Γ is given by

$$\Gamma \equiv \left\langle \delta b_r \int_{-\infty}^{\infty} v_{\parallel}\, \delta f\, dv_{\parallel} \right\rangle$$

$$= -\int_{-\infty}^{\infty} d\omega \sum_{m,n} \tau v_{the}^2 \frac{dn_o}{dr} \left\{ \left|\bar{b}_{mn}\right|^2 I_{mn} + c.c. \right\}$$

$$-\int_{-\infty}^{\infty} d\omega \sum_{m,n} v_{the}\, n_o \tau \frac{dv_{the}}{dr} \left\{ \left|\bar{b}_{mn}\right|^2 J_{mn} + c.c. \right\} \qquad (18)$$

where the integrals I_{mn} and J_{mn} are defined to be

$$I_{mn} = - \int_{-\infty}^{\infty} \frac{x\, e^{-\frac{x^2}{4}}}{\sqrt{2\pi}} \bar{W}(x,r)\, dx \,, \qquad J_{mn} = - \int_{-\infty}^{\infty} \frac{x\, e^{-\frac{x^2}{4}}}{\sqrt{2\pi}} \bar{Z}(x,r)\, dx \,. \quad (19)$$

The expression for Γ can be put in the following more transparent form,

$$\Gamma = - D_{\perp} \frac{dn_o}{dr} - L_T^n \frac{d\, T_{oe}}{dr} \,, \quad (20)$$

where the coefficients $D_{\perp}$ and L_T^n are given by

$$D_{\perp} = + 2v_{the}^2 \tau \int_{-\infty}^{\infty} d\omega \sum_{m,n} \left|\bar{b}_{mn}\right|^2 \text{Real } I_{mn}$$

(21)

$$L_T^n = + \frac{n_o \tau}{m_e} \int_{-\infty}^{\infty} d\omega \sum_{m,n} \left|\bar{b}_{mn}\right|^2 \text{Real } J_{mn} \,.$$

The test-particle energy flux takes the form $Q_{\perp} = < \delta b_r \int_{-\infty}^{\infty} \frac{m_e v_{\parallel}^3}{2} \delta f dv_{\parallel} >$, that is,

$$Q_{\perp} = - \int_{-\infty}^{\infty} d\omega \sum_{m,n} \frac{m_e v_{the}^2}{2} \tau \frac{dn_o}{dr} \left\{ \left|\bar{b}_{mn}\right|^2 2 \text{ Real } I'_{mn} \right\}$$

$$- \int_{-\infty}^{\infty} d\omega \sum_{m,n} \frac{m_e v_{the}^2}{2} \frac{n_o \tau}{2} \frac{d}{dr} v_{the}^2 \left\{ \left|\bar{b}_{mn}\right|^2 2\text{Real } J'_{mn} \right\} \,, \quad (22)$$

where

$$I'_{mn} = - \int_{-\infty}^{\infty} \frac{x^3 e^{-x^2/4}}{\sqrt{2\pi}} \bar{W}\,(x,r)\, dx \,, \qquad J'_{mn} = - \int_{-\infty}^{\infty} \frac{x^3 e^{-x^2/4}}{\sqrt{2\pi}} \bar{Z}\,(x,r)\, dx \,. \quad (23)$$

As before $Q_{\perp}$ can be written more transparently, as

$$Q_\perp = - L_n^T \frac{dn_o}{dr} - n_o \chi_\perp \frac{dT_{oe}}{dr} . \qquad (24)$$

$$L_n^T = + T_{oe} v_{the}^2 \tau \int_{-\infty}^{\infty} d\omega \sum_{m,n} \left|\bar{b}_{mn}\right|^2 \text{Real } I'_{mn} .$$

(25)

$$\chi_\perp = + \frac{v_{the}^2}{2} \tau \int_{-\infty}^{\infty} d\omega \sum_{m,n} \left|\bar{b}_{mn}\right|^2 \text{Real } J'_{mn} .$$

We note some important implications of the above formulae. Thus Eqs. (20), (21), (24) and (25) imply that even a single mode $\bar{b}_{mn}$ at a particular frequency ω (that is, a coherent mode) is capable of leading to non-zero radial transport. In order to understand this result, it is essential to bear in mind that the mode is not steady in the frame of reference of the background plasma. It should also be borne in mind that this complies with our assumptions that the test-particle trajectories described by Eqs. (1) & (2) would not in general lie on magnetic surfaces of the single mode in question. It is also important to note that in the first instance a time-dependent mode alters $\chi_\perp$ and $D_\perp$. Whether the global τ_{conf} is or is not affected depends on the extent of the localisation of the mode. Of course the formulae generally apply to an ensemble of modes which are not necessarily coherent. Furthermore, there are no convective contributions to the fluxes. In contrast to thermodynamics, the cross-coefficients L_T^n and L_n^T are not equal in general. Finally, we note that Eqs. (21) and (25) imply that $D_\perp$ is less than or of order $\chi_\perp$.

We derive some further consequences of the above theory. The test-particle density fluctuations $\delta n(r, \theta, t)$ can be written in analogy with Eq. (13)

$$\delta n = \int_{-\infty}^{\infty} d\omega \sum_{m,n} \bar{n}_{mn}(r, \omega) \, e^{i\left(m\theta + \frac{nz}{R} + \omega t\right)} \qquad (26)$$

where

$$\bar{n}_{mn}(r,\omega) = v_{the}\tau\, \bar{b}_{mn} \frac{dn_o}{dr} \frac{1}{\sqrt{2\pi}} \int_{-\infty}^{\infty} \bar{W}(x,\, r)\, e^{-\frac{1}{4}x^2}\, dx$$

$$+ \tau\, n_o(r)\, \bar{b}_{mn} \frac{dv_{the}}{dr} \frac{1}{\sqrt{2\pi}} \int_{-\infty}^{\infty} \bar{Z}(x,\, r)\, e^{-\frac{x^2}{4}}\, dx\ . \qquad (27)$$

Thus Eq. (27) expresses the density fluctuation amplitudes in terms of the magnetic amplitudes. If the profiles of mean quantities are known the integrals can be explicitly calculated by solving Eqs. (16) and (17), and Eq. (27) can be used to determine the field fluctuation spectrum if the density fluctuation spectrum is known.

It is also of interest to calculate the parallel heat flux vector in this model for a given mode m,n. Thus $\delta Q_{e\parallel}$ is given by

$$\delta Q_{e\parallel} = \int_{-\infty}^{\infty} \delta f\, \frac{m_e v_{e\parallel}^3}{2}\, dv_{e\parallel} \qquad (28)$$

whereas fluid theory (LIFSHITZ and PITAEVSKII, 1981) leads to the expression

$$\delta Q_{e\parallel} = -\, n_o\, \chi_{\parallel e} \left[ik_\parallel\, \bar{T}_{mn} + \bar{b}_{mn} \frac{dT_{oe}}{dr} + c.c.\right] + \delta U_\parallel\, n_o\, T_{oe} \qquad (29)$$

where $\chi_{\parallel e}$ is the parallel thermal diffusivity and $\delta U_\parallel$ is the parallel convective flow. The Fourier component of the temperature fluctuation is defined by

$$\bar{T}_{mn} = \frac{m_e v_{the}^3}{2n_o} \int_{-\infty}^{\infty} \bar{F}_{mn}\, x^2\, dx\ . \qquad (30)$$

Using Eq. (15) and comparing Eqs. (28) and (29), we obtain the following expressions for $\chi_{\parallel e}$ and $\delta U_\parallel$:

$$\chi_{\parallel e} = - \frac{\frac{v_{the}^2 \tau}{\sqrt{2\pi}} \int_{-\infty}^{\infty} x^3 \bar{Z} e^{-\frac{x^2}{4}} dx}{1 + \frac{ik_\parallel \tau v_{the}}{\sqrt{2\pi}} \int_{-\infty}^{\infty} x^2 \bar{Z} e^{-\frac{x^2}{4}} dx} \qquad (31)$$

and

$$\delta U_\parallel = \frac{v_{the}^2}{\sqrt{2\pi}\, n_o} \cdot \tau \bar{b}_{mn} \frac{dn_o}{dr} \left\{ \int_{-\infty}^{\infty} x^3 \bar{W} e^{-\frac{x^2}{4}} dx \right.$$

$$\left. + \frac{ik_\parallel \chi_{\parallel e}}{v_{the}} \int_{-\infty}^{\infty} x^2 \bar{W} e^{-\frac{x^2}{4}} dx \right\} . \qquad (32)$$

It is easily seen from Eqs. (16) and (17), that in the limit of high collisionality $\left(\tau << \frac{qR}{v_{the}}\right)$ $\chi_{\parallel e}$ approaches the Braginskii form $v_{the}^2 \tau$. The low collisionality limit must be handled more carefully. In this limit we require

$$\tau_{conf} >> \tau >> \frac{qR}{v_{the}} .$$

The above formulae then imply that $\chi_{\parallel e}$ is a function of m, n and ω and has both a real and imaginary part. A numerical study supplemented by a WKB method shows that the real part approaches a form conjectured previously by us (THYAGARAJA et al., 1980). We will discuss this in section 3.

3. EQUIVALENCE OF LANGEVIN AND FOKKER-PLANCK APPROACHES

We report in this section on some of our numerical results based on the above theory; details of the actual numerical methods are given in an appendix. Although some of the parameters chosen are typical of experiments, the emphasis of the present section is on demonstrating the equivalence of the Langevin and Fokker-Planck approaches. Accordingly the choice of parameters such as ρ and ε are largely dictated by numerical considerations.. In section 4 we shall apply the Fokker-Planck approach to conditions more relevant to TFR.

With the above caveats in mind we consider a periodic cylinder model of tokamak with minor radius a and periodicity length $2\pi R$. The mean magnetic field B_z is taken to be uniform and large compared with the poloidal field $B_{o\theta}(r)$ which is chosen so that $q = \frac{rB_z}{RB_\theta} = 1 + 2\frac{r^2}{a^2}$. For simplicity we consider only test-electron transport ignoring their energy transport. This is equivalent to assuming $T_{oe}(r)$ is uniform and equal to a fixed constant of order 1 keV. We also take the collision time τ to be uniform and constant. The spatial step-length ρ is also taken uniform and constant in such a way as to ensure that test-electron diffusion in the absence of magnetic fluctuations is finite but small compared with the expected diffusivity due to the presence of the mode or modes. The amplitude of the field fluctuations is prescribed as a function of r and t. The two principal conditions satisfied by these fluctuations apart from $\nabla \cdot \underline{B} = 0$, and periodicity in θ, z and t, are : $\frac{\delta B_r}{B_o} << 1$ and $\delta B_z = 0$. The forms of these will be given in the specific examples considered below.

With reference to the Fokker-Planck description, we note that in principle Eqs. (16) and (17) can be solved for arbitrary ω, m and n, exactly, if desired. But this exact solution is of little use in determining quantities such as $D_\perp$ and the test-electron density profile $n_o(r)$. For this reason we have chosen to solve Eqs. (16) and (17) numerically to obtain $\bar{W}$ and $\bar{Z}$ and evaluate $D_\perp$ by numerical integration. Assuming a uniform source of test-electrons $\dot{S}$, we then solve the transport equation

$$\frac{1}{r}\frac{d}{dr}\left(r\, D_\perp \frac{dn_o}{dr}\right) + \dot{S} = 0 \qquad (33)$$

with the boundary condition $n_o(a) = 0$ and $\frac{dn_o}{dr} = 0$ at $r = 0$. It is useful to remark that in the absence of magnetic fluctuations $\left(\frac{\delta B_r}{B_o} = 0\right)$ $D_{\perp o} = \frac{\rho^2}{4\tau}$ and n_o is a parabolic density profile.

In the Langevin approach, we consider a fixed number of test electrons, N say. At $t = 0$, these particles are introduced into the solution domain $0 < r < a$, $0 < \theta < 2\pi$, $0 < z < 2\pi R$, the distribution being uniform in space, and Gaussian in $v_\parallel$ with $\langle v_\parallel \rangle = 0$ and $\langle v_\parallel^2 \rangle \equiv v_{the}^2$. Using the numerical procedure described in the appendix, the finite difference forms of Eqs. (1) and (2) are solved for the ensemble of particles. During the course of such a solution, if a test-electron crosses the boundary $r = a$, it is reintroduced immediately into the solution domain as at $t = 0$. The numerical calculations show that after times $t \gtrsim \tau_{conf}$, the distribution of test-electrons to be steady except for statistical fluctuations due to the finiteness of N. Furthermore, the recycling rate of these particles is an outcome of the calculation. The recycling rate $\dot{N}$ is defined in terms of τ_{conf} as

$$\dot{N} = \frac{N}{\tau_{conf}} \ . \tag{34}$$

This is really an equation for τ_{conf} since the numerical simulation for fixed N yields $\dot{N}$. In order to compare the Fokker-Planck and Langevin approaches, it is useful to bear in mind the simple relations

$$N = 4\pi^2 R \int_o^a r n_o(r)\, dr$$

and

$$\dot{N} = \dot{S}\, 2\pi^2\, R\, a^2 \ . \tag{35}$$

With these definitions the diffusivity $D_{\perp o}$ in the absence of fluctuations is given by $\rho^2/4\tau$ and $\tau_{conf} = a^2/8D_{\perp o}$. In contrast to the Fokker-Planck approach, the Langevin approach does not require the smallness of $\delta B_r/B_o$. A more subtle restriction on the Fokker-Planck approach is that Eqs. (16) and (17) become singular at zero frequency and therefore are only valid for $\omega\tau_{conf} \gtrsim 1$. The Langevin approach suffers from no such restrictions and is valid at any frequency or collisionality. The only limitations are that the time-step Δt be sufficiently small and the number of test-electrons N be sufficiently large (for our purpose $N \sim 100$ and $\Delta t \sim 10^{-7}$ sec. suffices). In fact the relative error $\Delta\tau_{conf}/\tau_{conf}$

$\propto 1/\sqrt{N_{recyc}}$, where N_{recyc} is the total number of particles recycled and is given by $N t_{fin}$.

We first consider the effect of a single mode on test-electron transport. The purpose of this calculation is to compare the results of the Fokker-Planck approach with the Langevin approach. Table I gives the parameters.

Table I

Parameters		Values
R		150 cm
a		10 cm
v_{the}		10^9 cm s^{-1}
τ		10^{-6} s
ρ		1.0 cm
$\rho^2/4\tau$		2.5×10^5 cm^2 s^{-1}
τ_{conf}	(modes absent)	5×10^{-5} s
N	(Langevin)	128
Δt	(Langevin)	5×10^{-8} s
t_{fin}	(Langevin)	2.5 ms
Δr	(Fokker-Planck)	1.0 cm

We consider a single mode with m = 3 and n = 2 such that

$$\frac{\delta B_r}{B_o} = \frac{\varepsilon}{2} \left(\frac{r}{a}\right) \cos\left(m\theta - \frac{nZ}{R} + \omega t\right) . \qquad (36)$$

This corresponds to a magnetic fluctuation which would be produced typically by external currents, that is, not by the plasma itself. Of course, for the Monte Carlo calculation we also need to prescribe δB_θ (taking $\delta B_z = 0$) such that $\frac{1}{r}\frac{\partial}{\partial r}(r\delta B_r) + \frac{1}{r}\frac{\partial}{\partial \theta}\delta B_\theta = 0$. In Fig. 1a we present τ_{conf} obtained from the Fokker-Planck calculation as indicated in the procedure described above, with the parameters ε and ω varied. For $\varepsilon = 0$, we note that $\tau_{conf} = 5 \times 10^{-5}$ s as predicted by the exact solution in the presence of the "background" diffusivity $\rho^2/4\tau$. In Fig. 1b the analogous plot is derived from the Langevin/Monte Carlo

calculation. This shows that for amplitudes $\varepsilon \lesssim 7 \times 10^{-3}$, the two approaches are in agreement. Therefore, although it is not obvious from Figs. 1a and 1b, the differences from the "background" τ_{conf} at even moderate amplitudes $\varepsilon = 10^{-3}$ are significant. This has also been demonstrated in the Fokker-Planck code by reducing ρ and thereby decreasing the effect of the background.

We repeat this comparison for an "internal" 2,1 mode of the form

$$\frac{\delta B_r}{B_o} = \frac{\varepsilon}{2} \frac{r}{a} \exp\left[- (2 - q)^2 \right] \cos\left(m\theta - \frac{nZ}{R} + \omega t\right) . \qquad (37)$$

The results are presented in Figs. 2a and 2b, and demonstrate good agreement between the two methods, except for $\omega = 10^2$ and large amplitudes.

We now discuss interesting features of the properties of τ_{conf} as a function of ω and ε. With reference to Fig. 1a we note that at $\varepsilon = 3 \times 10^{-3}$, τ_{conf} as a function of ω has the following properties: For $\omega = 10^2$, τ_{conf} is hardly different from the background value. However, for $\omega > 10^6$ (when $\omega\tau > 1$) there is a very sharp reduction in τ_{conf}. This general pattern is also repeated at $\varepsilon = 5 \times 10^{-3}$ and $\varepsilon = 7 \times 10^{-3}$. Thus we conclude that even a single mode can alter test-electron transport by a factor of order two over the background value if the frequency of the mode ω is of the order of the collision frequency. The behaviour at increasing amplitude for a given frequency is fairly subtle, except when $\omega\tau \sim 1$, when the confinement time decreases with increasing amplitude. We note that the confinement time at fixed ω does not scale simply with ε^2. The main reason for this is that the diffusion coefficient $D_\perp$ includes the background diffusion $\rho^2/4\tau$. Turning to Figs. 2a and b we note that there is a clear degradation of confinement with increasing amplitude at fixed $\omega\tau$ and a resonant dip in confinement at $\omega\tau \sim 1$ at fixed amplitude. It is also of interest to note that the Fokker-Planck calculation apparently overestimates the confinement time at moderate to large amplitudes at low frequency relative to the Langevin code. The reason for this is that the Fokker-Planck takes only partial account of the island structure of the (2,1) mode and its possible

In addition, there is also the less important effect, of the neglect of the phase-shifts due to the background diffusion in the Fokker-Planck equation. These effects are fully represented in the Langevin code, bringing out the deterioration in confinement at low frequencies. Other calculations which we do not present show that at fixed $\omega\tau$ and ε, there is a similar resonant degradation in confinement when $\frac{v_{the}\,\tau}{qR} \sim 1$.

We now turn to an investigation of the effect of an ensemble of modes (many mode case). Before we describe the numerical experiments conducted, we wish to clarify certain points. In order to highlight the effect of an ensemble of modes in relation to the background transport, we have taken somewhat different values for the parameters. We choose ρ to be 0.2cm and $\tau = 3 \times 10^{-6}$sec, $\rho^2/4\tau = 3.3 \times 10^3$ $cm^2 s^{-1}$. If there were no modes in the system, and $v_{the} = 10^9$ cm s^{-1}, R = 50 cms and a = 10 cms, the confinement time is 3.75 msecs. It follows from Eq. (33) that, if in addition we prescribe a diffusivity $D_o = 10^6$ cm^2 s^{-1} for $\frac{r}{a} < 0.1$, τ_{conf} is not altered but the central density and profile for $\frac{r}{a} < 0.1$ certainly are. Inasmuch as we are interested in relatively short wavelength magnetic fluctuations, the effect of $m = 0$, $n = 0$ and $m = 1$ oscillations in the central region are schematically modelled by D_o . It is important to note that the main contribution of magnetic fluctuation induced transport comes from outside the central region and is expected to be much larger than $\rho^2/4\tau$. For ease of presentation we first turn to the Fokker-Planck results.

We take

$$\frac{\delta B_r}{B_o} = \frac{\varepsilon}{2} \sum_{m=1}^{10} \sum_{n=1}^{m} \frac{r}{a} \exp\left[-\frac{1}{4}(m - nq)^2\right] \cos\left(m\theta - \frac{nz}{R} + m\omega^* t\right) , \qquad (38)$$

where ω^* is of order the electron diamagnetic frequency and taken to be 3.3×10^5 and $\varepsilon = 10^{-3}$. The particle source $\dot{S}$ in Eq. (33) is taken uniform in r. Fig. 3 gives

$$\left\langle \left(\frac{\delta B_r}{B_o}\right)^2 \right\rangle = \left\{ \frac{\varepsilon^2}{8} \frac{r^2}{a^2} \sum_{m=1}^{10} \sum_{n=1}^{m} \exp\left[-\frac{1}{2}(m - nq)^2\right] \right\}^{1/2},$$

as a function of r/a, where we have deliberately chosen all the modes to vanish at $r = 0$. Fig. 4 gives the calculated values of $D_\perp(r)$ as a result of these fluctuations. Fig. 5 shows n_o as a function of r/a. Although $D_\perp$ is seen to be highly irregular, it results in a smooth $n_o(r)$ profile. The field fluctuations are important in the region $0.1 < \frac{r}{a} < 0.9$. The calculations show that $\tau_{conf} = 0.2$ msecs, and this is equivalent to a diffusivity of $\frac{a^2}{8\tau_{conf}}$, which is of order 5.0×10^4 $cm^2\ sec^{-1}$, well above the background diffusivity.

We have repeated the above calculation using the Langevin approach taking 64 particles and a time step of 5×10^{-8}s, running the code for a time $\tau_{fin} = 2.0$ msecs. The confinement time of 0.2 msecs agrees with the result of the Fokker-Planck calculation. We have also repeated the calculation with $\omega^* = 0$ keeping all other parameters fixed. The confinement time in this case is 0.4 msecs. This calculation has no analogue in the Fokker-Planck approach.

It is of interest to compare the above results obtained from the test-particle approach to the estimates derivable from our earlier two-fluid approach (HAAS and THYAGARAJA, 1984) for the same conditions. Two-fluid theory gives $\chi_{\perp e} \sim \frac{(2\pi R)^2}{\tau_e} \varepsilon^2 \simeq 3 \times 10^4\ cm^2 s^{-1}$ and $\tau_{conf} = \frac{a^2}{8\chi_\perp} \simeq 0.3$ msec. This is of the same order as the results quoted for both the Fokker-Planck and Langevin approaches. $\chi_{\perp e}$ calculated from the RECHESTER and ROSENBLUTH (1978) formula $\chi_{\perp e} \sim qR\, v_{the}\, \varepsilon^2$ is of order $1.5 \times 10^5\ cm^2\ s^{-1}$, implying $\tau_{conf} \sim 8.0 \times 10^{-2}$ msecs.

4. APPLICATION TO TFR

In this section we consider an application of the present model of anomalous transport to TFR (EQUIPE TFR, 1983). This work relates to high

m,n density fluctuations and anomalous electron thermal conduction. We note that the density fluctuations observed are apparently consistent with certain general features of drift waves, but have been found incapable of predicting the radial dependence of $\chi_{\perp e}(r)$ as obtained in experiment. We give below an outline of a magnetic fluctuation interpretation of the same data. We do not enquire as to the origins of the fluctuations (drift waves or otherwise) but take them as specified below. Here we make the explicit assumptions that the expressions for $\chi_\perp$ and $\delta n/n$ calculated in terms of $\delta B_r/B_o$ for test-electrons apply to the plasma electrons; we discuss this further in section 5.

As before we represent $\frac{\delta B_r}{B_o}$ as a function of position and time by the expression,

$$\frac{\delta B_r}{B_o} = \frac{\varepsilon r}{2a} \sum_{m=1}^{m_{max}} \sum_{n=1}^{m} e^{-\frac{1}{4}(m-nq)^2} \cos\left(m\theta - \frac{nZ}{R} + m\,\omega^* t\right) \qquad (39)$$

Choosing

$$q(r) \equiv 1 + 3\frac{r^2}{a^2},$$

$\varepsilon = 3 \times 10^{-5}$, $\omega^* = 8$ kHz (5×10^4 rads sec^{-1}), R = 100 cms, a = 20 cms, we model the effect of a large number of resonant modes with frequencies in the range 10-1,000 kHz and $k_\theta \sim k_r \sim \frac{m}{a}$. Provided we choose $m_{max} \sim 100$ the calculations are not sensitive to this quantity, which in the particular instance given below is taken to be 80. In order to estimate the transport, we further assume that the Braginskii collision time $\tau = 10^{-6}$sec and $v_{the} = 10^9$ cm sec^{-1}, both taken to be uniform in r. These conditions approximate fairly closely to the experiment. Since the value of ε is reasonably small, we have used the Fokker-Planck approach, with a "background" diffusivity $\frac{\rho^2}{4\tau} \sim 600$ cm^2 s^{-1}, well below the measured experimental $\chi_{\perp e}$ values and of order the ion neoclassical conductivity. The results of this calculation are given in Figs. 6a and b. Fig. 6a gives the calculated value of $\chi_{\perp e}$ (see Eq. (25)) as a

function of r. At $\frac{r}{a} = 0.5$, $\chi_{\perp e} = 3 \times 10^3$ cm^2 s^{-1}, the same as in the experiment. This has been used to fix the assumed value of ε, there being no other free parameters. Both the profile of $\chi_{\perp e}$ and the numerical values agree with the experimental values of $\chi_{\perp e}$ for all larger radii (see Fig. 14 of TFR paper). For $\frac{r}{a} < 0.5$ the calculated $\chi_{\perp e}$ falls away steadily to zero, whereas the observed $\chi_{\perp e}$ has a minimum and rises again towards the magnetic axis. This is merely an artefact of our neglecting sawteeth and associated low mode activity in the vicinity of the $q = 1$ surface. It should also be noted that the "spikeyness" of the calculated $\chi_{\perp e}$ profile is again an artefact due to the low-order modes in Eq. (39). Substitution of such an $\chi_{\perp e}(r)$ in a transport equation always leads to smooth T_e profiles which are flattened in the vicinity of the largest spikes. Fig. 6b shows a plot of $\sqrt{\left(\frac{\delta n}{n_o}\right)^2}$ as a function of $\frac{r}{a}$ as calculated from Eqs. (27) and (39) assuming $\frac{1}{no}\frac{dn_o}{dr} = 4\left(\frac{r}{a}\right)$. We note that from $\frac{r}{a} = 0.1$ to $\frac{r}{a} = 1.0$ the curve is almost linear as indicated by experiment. The value at $\frac{r}{a} = 0.5$ is 0.1% which is a factor of two lower than indicated by experiment, but consistent with the measured accuracy. The corresponding magnetic fluctuation intensity which is $\sqrt{\left(\frac{\delta B_r}{B_o}\right)^2}$ is 5×10^{-5}.

We next address certain interesting features observed in the TFR experiment relating to the time variation of $\chi_{\perp e}$, $\frac{\delta n}{n_o}$, n_o during the flat-top phase as shown in Figs. 8, 10 and 12 in the TFR paper. It is seen from Fig. 8 of TFR paper that from 100-200 msecs the current and the absolute level of the density fluctuations $\langle(\delta n)^2\rangle$ remain approximately constant while the density rises by 100%. This is also confirmed by Fig. 10, where during the corresponding period $\frac{\delta n}{n_o}$ falls linearly with time. Fig. 12 shows that this is correlated with a sharp decrease of $\chi_{\perp e}$. We have attempted to simulate this behaviour as follows. We have performed a series of calculations in which v_{the}, q and ω^* are held fixed. The variation of mean density is simulated by taking a series of values for

the collision time τ. We have also slightly altered the representation of $\frac{\delta B_r}{B_o}$ in Eq. (39). Thus

$$\frac{\delta B_r}{B_o} = \frac{r}{2a} \sum_{m=1}^{m_{max}} \sum_{n=1}^{m} \varepsilon_{mn} e^{-\frac{1}{4}(m-nq)^2} \cos\left(m\theta - \frac{nZ}{R} + m\omega^* t\right) \qquad (40)$$

where the parameters ε_{mn} are now chosen so that the amplitude of the m,n^{th} Fourier component is proportional to $\frac{1}{m}$ corresponding to the experimental statement that $\frac{\delta n}{n_o} \sim \frac{1}{k_\perp L_n}$; this choice results in a linearly rising radial profile for $\frac{\delta n}{n_o}$, the values of which depend on the mean[a] density n_o. The results of this density variation at a particular point $\frac{r}{a} = 0.7$ are shown in Figs. 7a, b, c. Fig. 7a shows the assumed variation of $\sqrt{\left(\frac{\delta n}{n_o}\right)^2}$ evaluated at $r = 0.7a$ with the collision frequency τ^{-1} which is proportional to the mean density n_o. Note that we have deliberately chosen a rather wide variation of τ^{-1} spanning the experimental region. Fig 7b shows the resulting variation of $\sqrt{\left(\frac{\delta B_r}{B_o}\right)^2}$ at the same radius. It is seen clearly that over this range of variation, $\frac{\delta n}{no}$ and $\frac{\delta B_r}{B_o}$ are simply proportional to each other to a good approximation. Thus for the conditions of TFR the variation of $\frac{\delta n}{n_o}$ and $\frac{1}{n_o}$ implies, according to our model, $\frac{\delta B_r}{B_o} \propto \frac{1}{n_o}$. Fig. 7c shows the value of $\chi_{\perp e}$ calculated at the same point as a function of the collision frequency. It follows from Fig. 7c that over the range of collision frequencies considered, $\chi_{\perp e} \propto \frac{1}{n_o}$, as suggested by the TFR results.

An interesting implication of the above results (at $r = 0{\cdot}7a$) is that for the TFR experiment at least, $\chi_{\perp e} \sim \chi_{\parallel e} \left(\frac{\delta B_r}{B_o}\right)^2$, with $\chi_{\perp e} \propto \frac{1}{n_o}$

and $\frac{\delta B_r}{B_o} \propto \frac{1}{n_o}$, implies $\chi_{\parallel e} \propto \frac{(2\pi R)^2}{\tau}$ and not $\chi_{\parallel e} \propto v_{the}^2 \tau$ or $\chi_{\parallel e} \propto 2\pi R\, v_{the}$. This can also be directly demonstrated from our results to hold for each value of r. Thus Fig. 8 shows the ratio of the effective value of $\chi_{\parallel e}$ obtained from Eq. (31) and averaged over all the modes present, to the quantity $\frac{(2\pi R)^2}{\tau}$ as a function of $\frac{r}{a}$. It is that this quantity varies between 0.5 and 2.0 across the plasma. Thus the test-particle calculation appears to confirm a global scaling conjectured by us based on ALCATOR and other ohmic experiments (COOK et al., 1982). It is also interesting to note that if it is assumed that $\sqrt{<(\delta n)^2>}$ is more or less constant from the q = 1 surface to the edge, then $\chi_{\perp e}$ is proportional to $\frac{1}{n_o(r)}$. In more collisional conditions where $\chi_{\parallel e} \propto v_{the}^2 \tau$, the magnetic fluctuation theory can account for the scaling $\chi_{\perp e} \propto \frac{1}{n_o}$, if, and only if, $\frac{\delta B_r}{B_o}$ is independent of n_o.

5. DISCUSSION

We now discuss a number of points raised by the proposed model of test-electron transport due to magnetic fluctuations. Although we have formulated the model for test-electrons, the calculations apply with suitable modification to any other test-charges. Addressing the question is test-electron transport indicative of plasma transport? - the following comments are in order : The plasma electrons respond to $\underline{E}$ and $\underline{B}$ fields according to the exact Fokker-Planck equation

$$\frac{\partial f_e}{\partial t} + \underline{v}\cdot\nabla f_e - \frac{e}{m_e}\left(\underline{E} + \frac{\underline{v}\times\underline{B}}{c}\right)\cdot\nabla_v f_e = C(f_e, f_e) + C(f_e, f_i) + \bar{S} \quad . \quad (41)$$

Eq. (3) which is satisfied by the test-electron distribution function can be "derived" from Eq. (41) by approximating the collision terms drastically to preserve only their essential properties (parallel velocity relaxation and spatial diffusion $\rho^2/4\tau$) and by averaging over velocities in the plane perpendicular to the instantaneous field line. These approximations alone would not quite yield Eq. (3), but a slightly

more general form in which $v_{\parallel}\underline{b}$ in Eq. (3) is replaced by $v_{\parallel}\underline{b} + \underline{v}_{drift}(\underline{r}, t)$ where $v_{drift}(r, t)$ is in lowest-order given by

$$\underline{v}_{drift} = - \frac{c}{B^2} \left(\underline{E} + \frac{\nabla p}{en} \right) \times \underline{B} ,$$

where p and n are the test-electron pressure and density respectively. In addition the force term $- \frac{e}{m_e} E_{\parallel} \frac{\partial f_e}{\partial v_{\parallel}}$ will have to be included. Taking a suitable gauge, it is easy to extend our Fokker-Planck treatment to cover this case.

Taking full account of the electric fields in the Langevin treatment, it is easily seen that Eq. (1) must be replaced by

$$\frac{d\underline{r}}{dt} = v_{\parallel} \underline{b} + c \frac{\underline{E} \times \underline{B}}{B^2} + \underline{c}_{\perp} (\omega_{ce} t) ,$$

where $|\underline{c}_{\perp}|$ is of order v_{the} and $\underline{c}_{\perp}$ is a rapidly rotating vector perpendicular to $\underline{b}$. Eq. (2) is replaced by

$$\frac{dv_{\parallel}}{dt} + \frac{v_{\parallel}}{\tau} = R(t) - \frac{e}{m_e} E_{\parallel}(t) .$$

It is easily seen that the full effect of the $\underline{c}_{\perp}$ term is included in our present description if we take ρ_e to be the electron larmor radius v_{the}/ω_{ce} . For typical tokamak conditions the velocity $c \frac{\underline{E} \times \underline{B}}{B^2}$ is much smaller than $v_{\parallel} \sim v_{the}$. Also for the frequencies considered $v_{the} >> \frac{eE_{\parallel}}{m_e \omega}$. In any event a theory including the full electric field can only be compared to experiment if at least two fluctuating quantities are simultaneously known, $\delta n/n$ and $\delta T_e / T_{oe}$, say. We note also that a different interpretation from the one given above can be attached to the spatial step ρ . Thus $\rho^2/4\tau$ can be used to represent phenomenologically all other transport processes neglected in the present theory.

For example, the transport due to a single-mode can be interpreted as relative to all other transport processes (described by $\rho^2/4\tau$). In the second interpretation ρ need not be the electron Larmor radius.

The crucial difference between the plasma electrons and the test-electrons is that the test-electrons respond to given $\underline{E}$ and $\underline{B}$ fields, whereas the plasma electrons together with the ions, self-consistently determine the $\underline{E}$ and $\underline{B}$ fields. If $\underline{E}$ and $\underline{B}$ are completely known from experiment and are of small amplitude, the test-electron response is the same as the plasma response. To the extent that experiment does <u>not</u> give such detailed information, the test-electron transport determined by our model can at best represent plasma transport in a schematic way. It is of interest to observe that several general features of our test electron results appear to resemble gross features of experimental plasma transport.

We regard the present work as an extension in one sense of our earlier two-fluid turbulence interpretation. In the fluid theory, $\chi_{\parallel e}$ is a prescribed quantity, especially at low collisionality. Given expressions for $\chi_{\parallel e}$ we were able to derive effective perpendicular transport coefficients in the presence of electromagnetic fluctuations. In the present work no assumptions have been made about collisionality other than $\frac{\tau}{\tau_{conf}} << 1$. This, in fact, is no more than assuming $\left\langle \left(\frac{\delta B_r}{B_o}\right)^2 \right\rangle << \frac{a^2}{v_{the}^2 \tau^2} \sim 10^{-5}$. Under these conditions we have explicitly evaluated the parallel transport and shown that $\chi_{\parallel e}$ is indeed reduced relative to $v_{the}^2 \tau$ as we had assumed in our fluid theory.

Finally, we note that some of our results, especially the maximum transport at $\omega\tau \sim 1$ and $\frac{v_{the}\,\tau}{qR} \sim 1$, are similar to those obtained by YAMAGISHI and BHADRA (1983). Their model is for a system with homogeneous turbulence. Our model is also different from the theory due to RECHESTER and ROSENBLUTH (1978) and expounded by KROMMES et al.(1983). In this double diffusion theory, the effective perpendicular transport of

test-electrons is, in the low collisionality regime, the result of parallel convection at v_{the} and stochastic field diffusion due to overlap of stationary islands. This theory apparently does not lead to transport from a single mode - time-dependent or stationary. Whereas in this theory the ergodisation of field lines is explicitly due to island overlap, the particle trajectories described by our Langevin equation, Eq. (1), are in general ergodic, irrespective of whether the instantaneous field lines are ergodic or not. Furthermore, collisions play an essential rôle in our theory, despite the fact that $\frac{v_{the}\,\tau}{qR}$ and $\omega\tau$ are sometimes much larger than unity, for the important reason that $\frac{\tau}{\tau_{conf}} \ll 1$, as is true in actual experiments.

6. CONCLUSIONS

The specific conclusions of our calculations have already been listed in the introduction. More generally, the test-particle model is effective in calculating parallel transport at arbitrary collisionality in the presence of magnetic field fluctuations. In this sense, it extends and justifies our earlier two-fluid approach to anomalous transport in tokamaks. We note, however, that the two-fluid approach is better able to take account of quasineutrality and its consequences for particle transport. Thus the two-fluid theory (HAAS and THYAGARAJA, 1984) suggests that particle and energy fluxes have in general convective contributions which may be inward depending on the conditions. Experiment is known to be in agreement with this prediction of two-fluid theory (COPPI and SHARKY, 1981). Thus the present level of test-particle theory complements rather than includes the two-fluid interpretation of anomalous transport.

REFERENCES

COOK I., HAAS F.A. and THYAGARAJA A. (1982) Plasma Physics 24, 331.

COPPI B. and SHARKY N. (1981), Nucl. Fusion 21, 1363.

EQUIPE TFR (1983), Plasma Physics 25, 641.

HAAS F.A. and THYAGARAJA A. (1984) Plasma Physics 26, 641.

KROMMES J.A., OBERMAN C. and KLEVA R.G. (1983) Journal of Plasma Physics 30, 11.

LIFSHIFTZ E.M. and PITAEVSKII L.P. (1981) Physical Kinetics, Pergamon Press, Oxford, Section 58.

RECHESTER A.B. and ROSENBLUTH M.N. (1978) Phys. Rev. Letts. 40, 38.

THYAGARAJA A., HAAS F.A. and COOK I. (1980), Nucl. Fusion 20, 611.

UHLENBECK G.E.,and ORNSTEIN L.S. (1930), Reprinted in Selected Papers on Noise and Stochastic Processes, edited N. Wax, Dover Publications, New York, 1954.

VAN KAMPEN N.G. (1983), Stochastic Processes in Physics and Chemistry, North Holland Publishing Co., Oxford, p. 209.

YAMAGISHI T. and BHADRA D.K. (1983) Plasma Physics 25, 1414.

APPENDIX

The numerical treatment of the Fokker-Planck formulation is straightforward. As noted in the text, Eqs. (16) and (17) can be solved in terms of Weber functions analytically, but this solution is not useful. Instead, we choose an x interval $[-7.5, 7.5]$ and finite-difference the equations. Centred-differencing gives a tri-diagonal matrix (inhomogeneous) system. Applying the boundary conditions $\bar{W}, \bar{Z} = 0$ at both end points, the system is solved by standard methods. This procedure is repeated at each spatial grid point r_i, using the appropriate values of ω, $k_\parallel$ etc. for all the modes present. Calculating $D_\perp(r_i)$ in this way, we finally solve for $n_o(r_i)$. Since the test-particle sources are specified, $n_o(r)$ is obtained by two quadratures. Typically, we find that 51 equally spaced mesh points in the x (i.e. velocity) space and a similar number of r-grid points give adequate accuracy.

The numerical analysis of the Langevin equations (1) and (2) requires more work. Using the tokamak ordering $B_{oz} >> B_\theta$, B_r and $\delta B_z = 0$, the equations of motion are written in terms of non-dimensional variables as follows:

$$\frac{dI}{dt} = -\frac{\varepsilon v_\parallel}{a}\frac{\partial \Psi}{\partial \theta}(I, \theta, \phi, t)$$

$$\frac{d\theta}{dt} = \frac{v_\parallel}{q(I)R} + \frac{\varepsilon v_\parallel}{a}\frac{\partial \Psi}{\partial I}(I, \theta, \phi, t) \qquad \text{(A.1)}$$

$$\frac{d\phi}{dt} = \frac{v_\parallel}{R}$$

where

$$I \equiv \frac{1}{2}\frac{r^2}{a^2}, \quad \phi = \frac{z}{R}, \quad q = \frac{rB_{oz}}{RB_{o\theta}},$$

$$\delta b_r = -\frac{\varepsilon}{r}\frac{\partial \Psi}{\partial \theta} \qquad \text{(A.2)}$$

$$\delta b_\theta = \varepsilon \frac{\partial \Psi}{\partial r}$$

We take $q(I) \equiv 1 + 4I$. The poloidal flux function Ψ takes the form,

$$\Psi \equiv \sum_m \sum_n F_{mn}(I) \cos (m\theta - n\phi + m\omega_* t) \qquad (A.3)$$

F_{mn} can be arbitrary smooth functions such that $F_{mn}(o) = 0$.

The equation for ϕ is trivially solved. In order to calculate the motion between collisions, the equations (A.1) must be cast in suitable finite-difference forms and solved. Clearly they imply the area-preserving property,

$$\frac{\partial\big(I(t),\ \theta(t)\big)}{\partial\big(I(o),\ \theta(o)\big)} = 1 \qquad (A.4)$$

Denoting $I(t + \Delta t)$ by I' and $\theta(t + \Delta t)$ by θ' , the following implicit-finite difference equations are derived from (A.1) using a Picard iteration.

$$I' = I + \frac{\varepsilon\, v_\parallel}{a} \sum_{m,n} F_{mn}(I')\, m \int_t^{t+\Delta t} \sin\Big(m\theta_o(u) - n\,\frac{v_\parallel u}{R} + m\omega_* u + \Phi_o\Big)\, du$$

$$\theta' = \theta + \frac{\Delta t\, v_\parallel}{q(I')R} + \frac{\varepsilon\, v_\parallel}{a} \sum_{m,n} \frac{dF_{mn}}{dI'} \int_t^{t+\Delta t} \cos\Big(m\theta_o(u) - n\,\frac{v_\parallel u}{R} + m\omega_* u + \Phi_o\Big)\, du \qquad (A.5)$$

where

$$\Phi_o \equiv m\theta(t) - n\phi(t) + \omega_* m t\ , \quad \theta_o(u) = \frac{u\, v_\parallel}{q(I')R} .$$

These implicit equations are iteratively solved for I', θ' given I, θ, ϕ and t . It is easy to prove that the exact solution of (A.5) satisfies

$$\frac{\partial(I', \theta')}{\partial(I, \theta)} = 1 \ .$$

These methods can be readily extended to situations in which $\delta B_z \neq 0$ (these are more relevant to reversed field pinch applications).

The Langevin equation (2) is written in the finite-difference form,

$$v_{\parallel}(t + \Delta t) = \left\{ \frac{1 - \frac{\Delta t}{2\tau}}{1 + \frac{\Delta t}{2\tau}} \right\} v_{\parallel}(t) + \bar{R} \left\{ \frac{\Delta t}{1 + \frac{\Delta t}{2\tau}} \right\}. \qquad (A.6)$$

If we choose $\bar{R}$ from a Gaussian with zero mean and

$$\langle \bar{R}^2 \rangle = \frac{2 \, v_{the}^2}{\tau \, \Delta t} \ ,$$

$$\langle v_{\parallel}(t + \Delta t) \rangle = \left\{ \frac{1 - \frac{\Delta t}{2\tau}}{1 + \frac{\Delta t}{2\tau}} \right\} \langle v_{\parallel} \rangle \ .$$

Provided $\frac{\Delta t}{2\tau} < 1$, $\langle v_{\parallel}(t) \rangle \to 0$ irrespective of $\langle v_{\parallel}(o) \rangle$. If at each time-step R is chosen in the above way (i.e. uncorrelated with the previous values, fulfilling the Markoff property), then

$$\langle v_{\parallel}^2(t) \rangle = v_{the}^2 \quad \text{for sufficiently large } t \ .$$

Furthermore the $v_{\parallel}$'s will be Maxwell distributed. The random spatial jumps are taken with the length $\rho\left(\frac{\Delta t}{\tau}\right)^{1/2}$ at <u>every</u> time step prior to the deterministic integration for each particle. This procedure captures the essence of the 'persistent' collision effect of the Fokker-Planck equation rather well. It should be noted that in the text - for conceptual simplicity - it was stated that a random spatial step of length ρ is taken at each collision, rather than at each time-step. All calculations are vectorised and $\varepsilon \, v_{\parallel} \frac{\Delta t}{a}$ chosen sufficiently small ($\sim 10^{-4}$) to ensure accuracy.

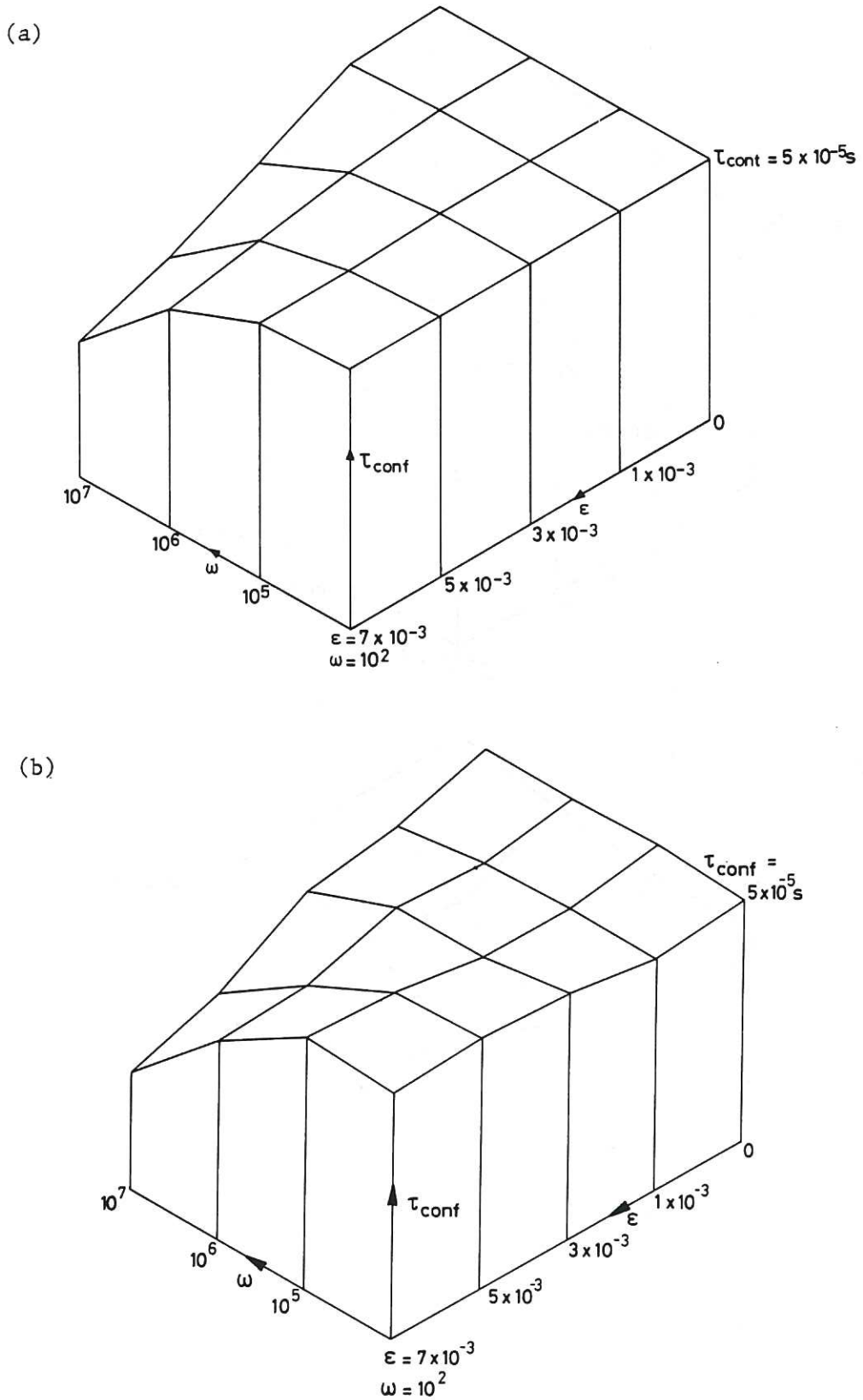

Fig. 1 Plot of confinement time (τ_{conf}) versus mode frequency (ω) and amplitude (ϵ). Note τ_{conf} is linear in scale and the interval $\epsilon = 0 - 1 \times 10^{-3}$ is not to scale.
(a) Fokker-Planck, external (3,2) mode.
(b) Langevin, external (3,2) mode.
For both cases τ_{conf} (background) = 5×10^{-5}s.

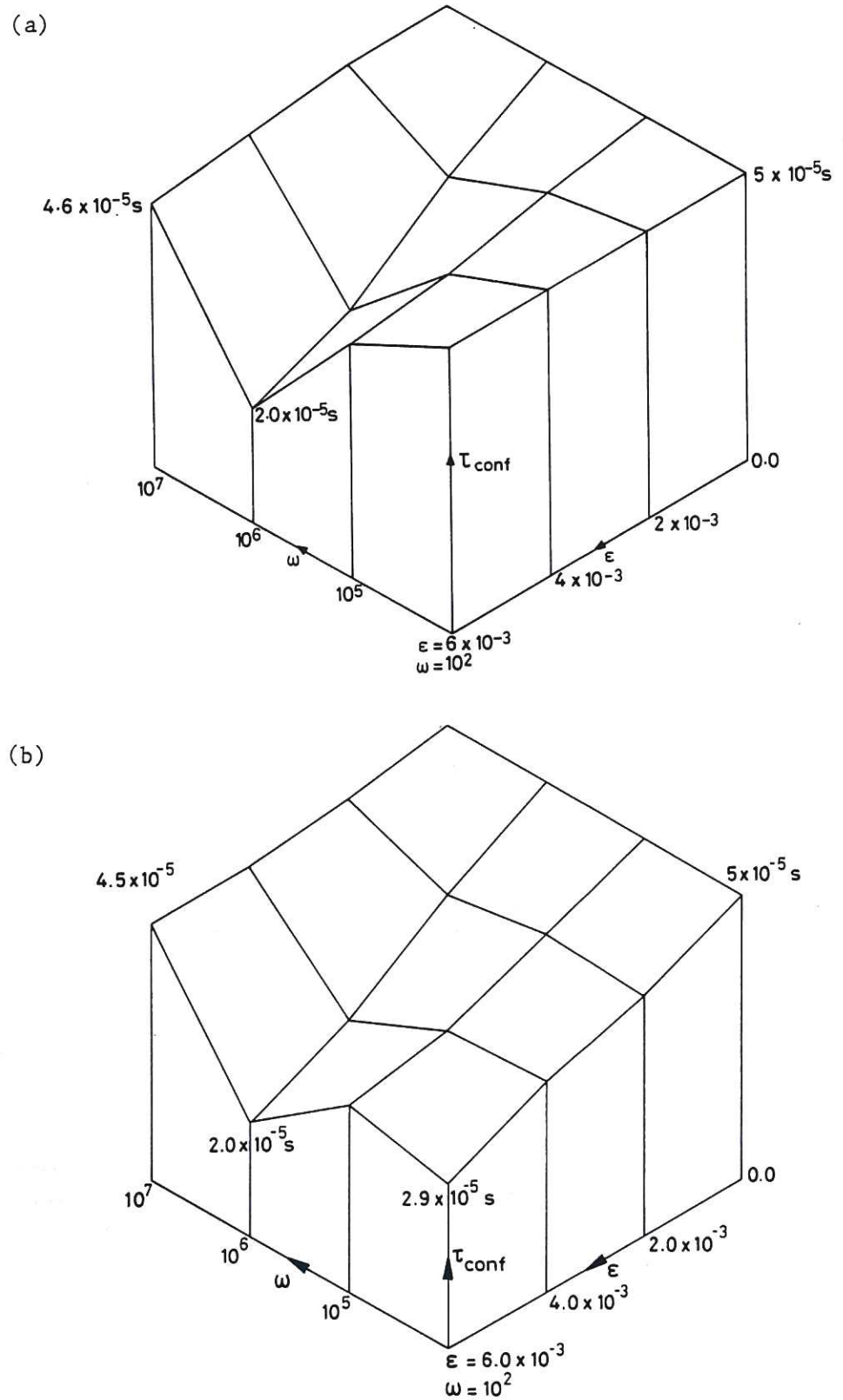

Fig. 2 Plot of confinement time (τ_{conf}) versus mode frequency (ω) and amplitude (ϵ). Note τ_{conf} is linear in scale.
(a) Fokker-Planck, internal (2,1) mode.
(b) Langevin, internal (2,1) mode.
For both cases τ_{conf} (background) = 5×10^{-5}s.

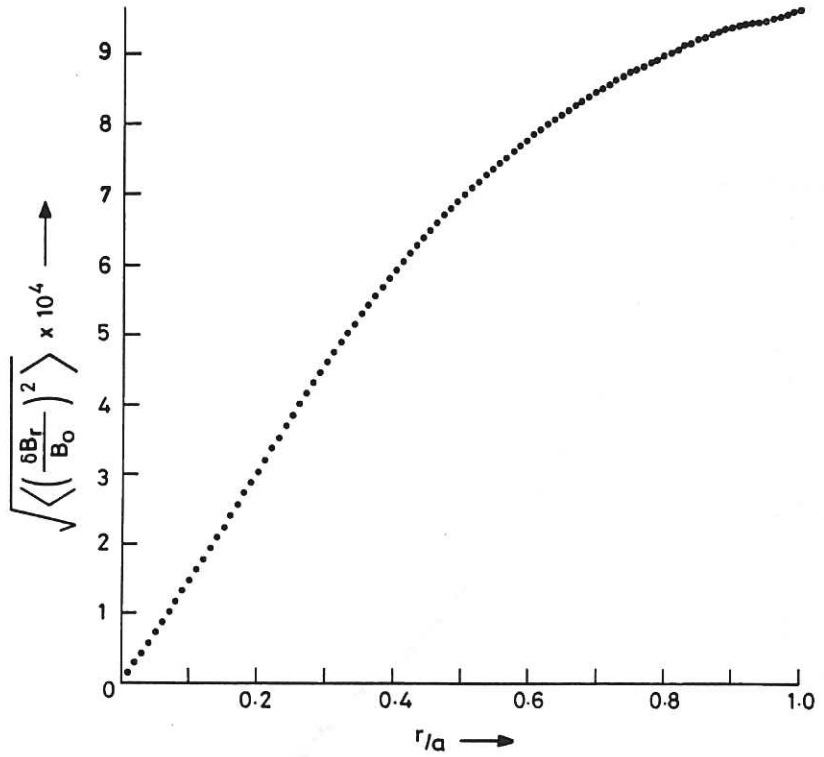

Fig. 3 Radial profile of magnetic fluctuation level $\sqrt{(\delta B_r/B_0)^2}$: $\epsilon = 10^{-3}$, $m_{max} = 10$ (see Eq. [38]).

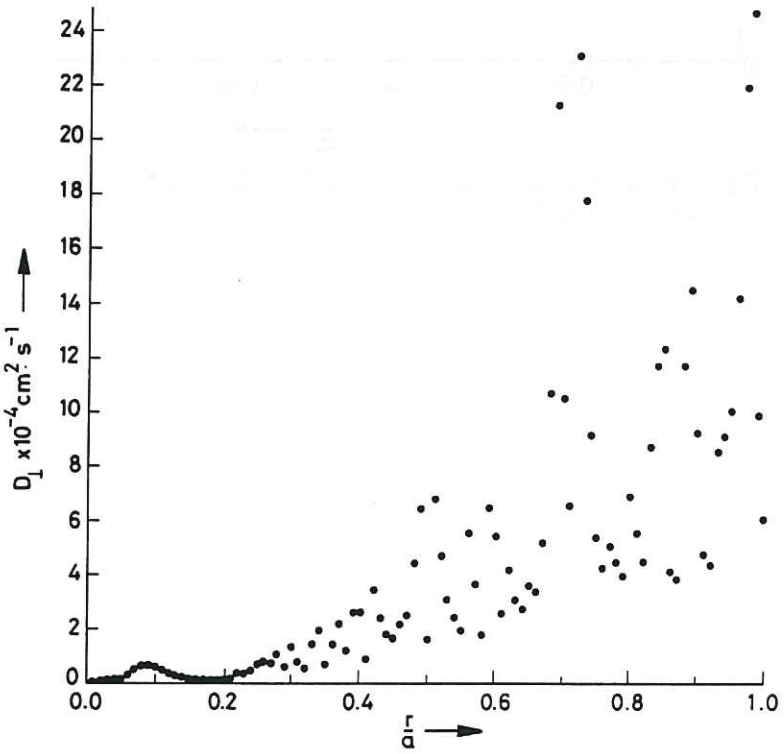

Fig. 4 Radial profile of magnetic turbulence induced diffusion coefficient ($D_\perp$ [r/a]), calculated for the fluctuation intensity given in Fig. 3.

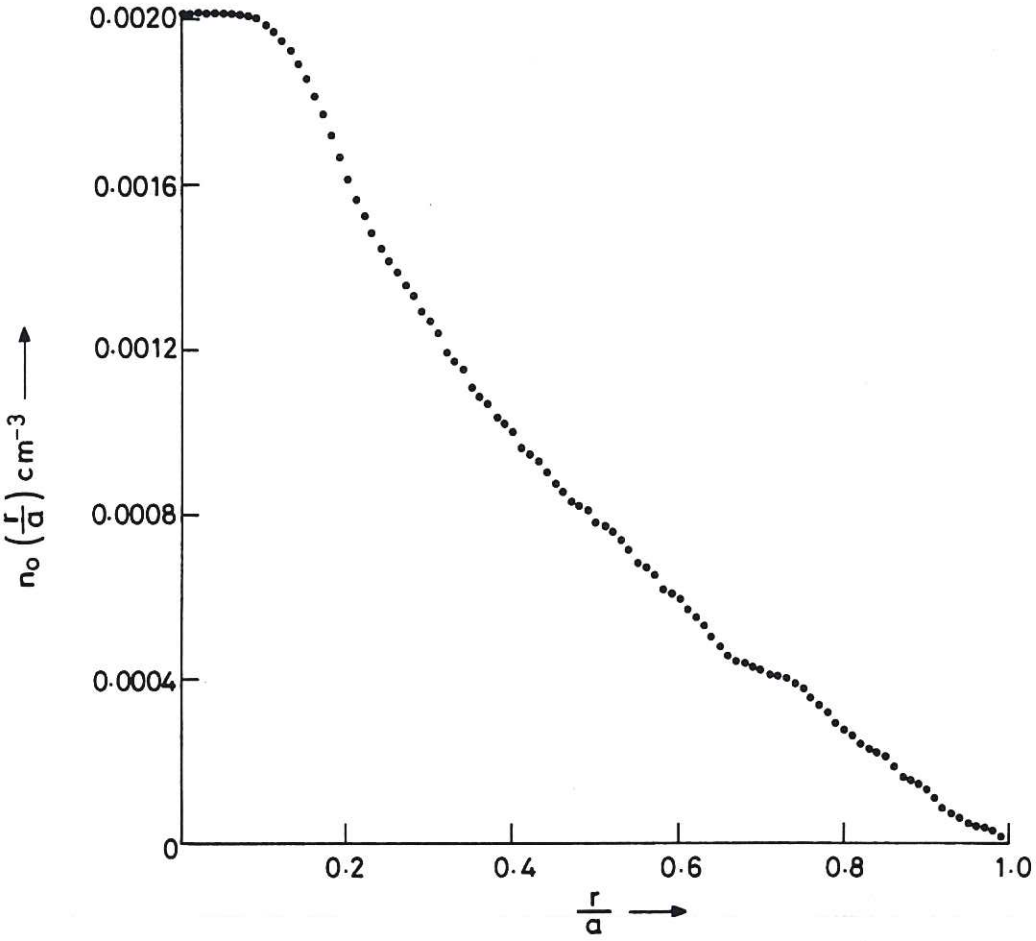

Fig. 5 Radial profile of $n_0(r/a)$ (from Eq. [33]) for the same conditions as Fig. 3.

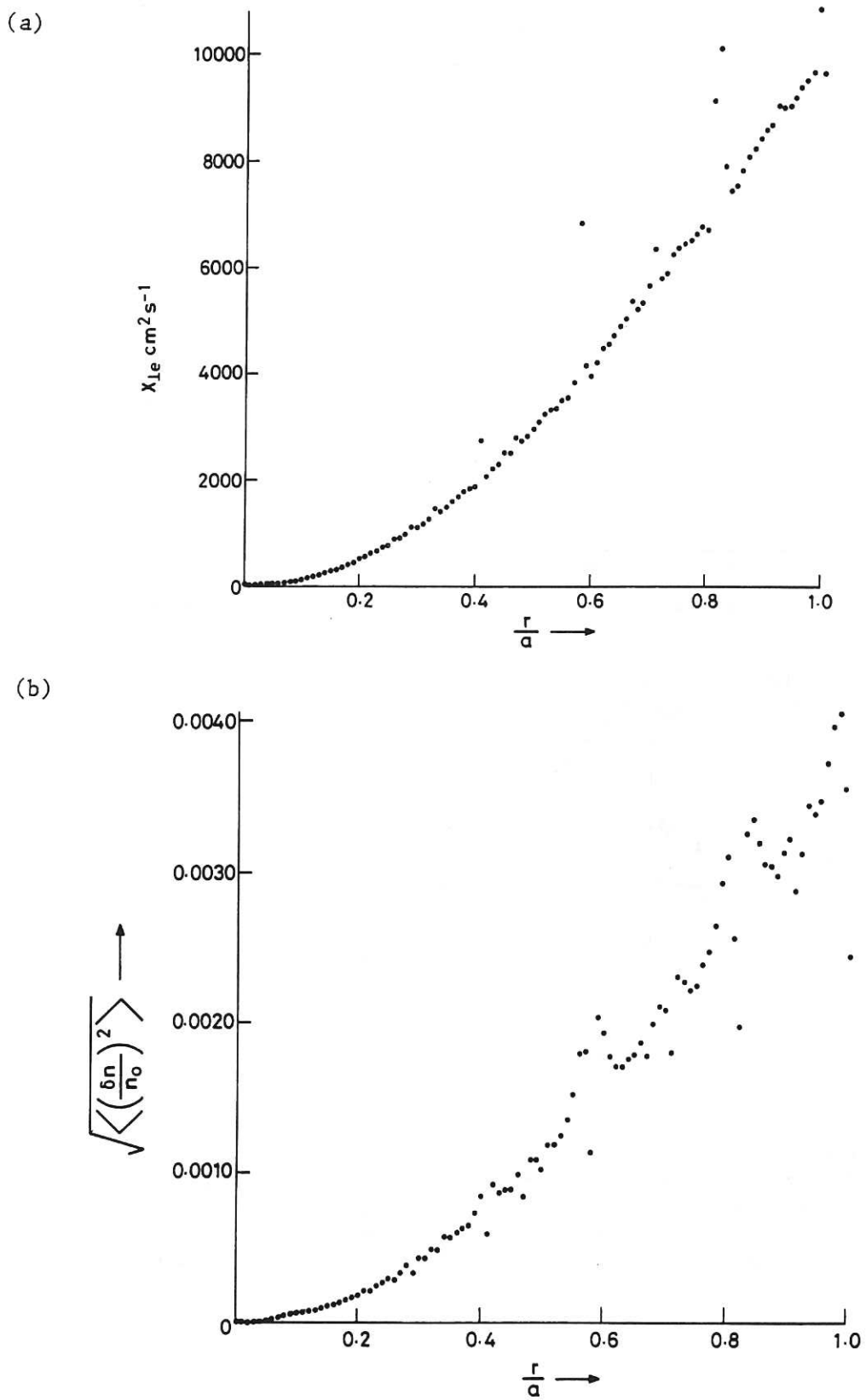

Fig. 6 Radial profiles of magnetic fluctuation induced quantities for TFR:
(a) thermal diffusivity $\chi_{\perp e}(r/a)$.
(b) RMS density fluctuation $\sqrt{(\delta n/n_0)^2}$. These are calculated from $\delta B_r/B_0$ given by Eq.(39).

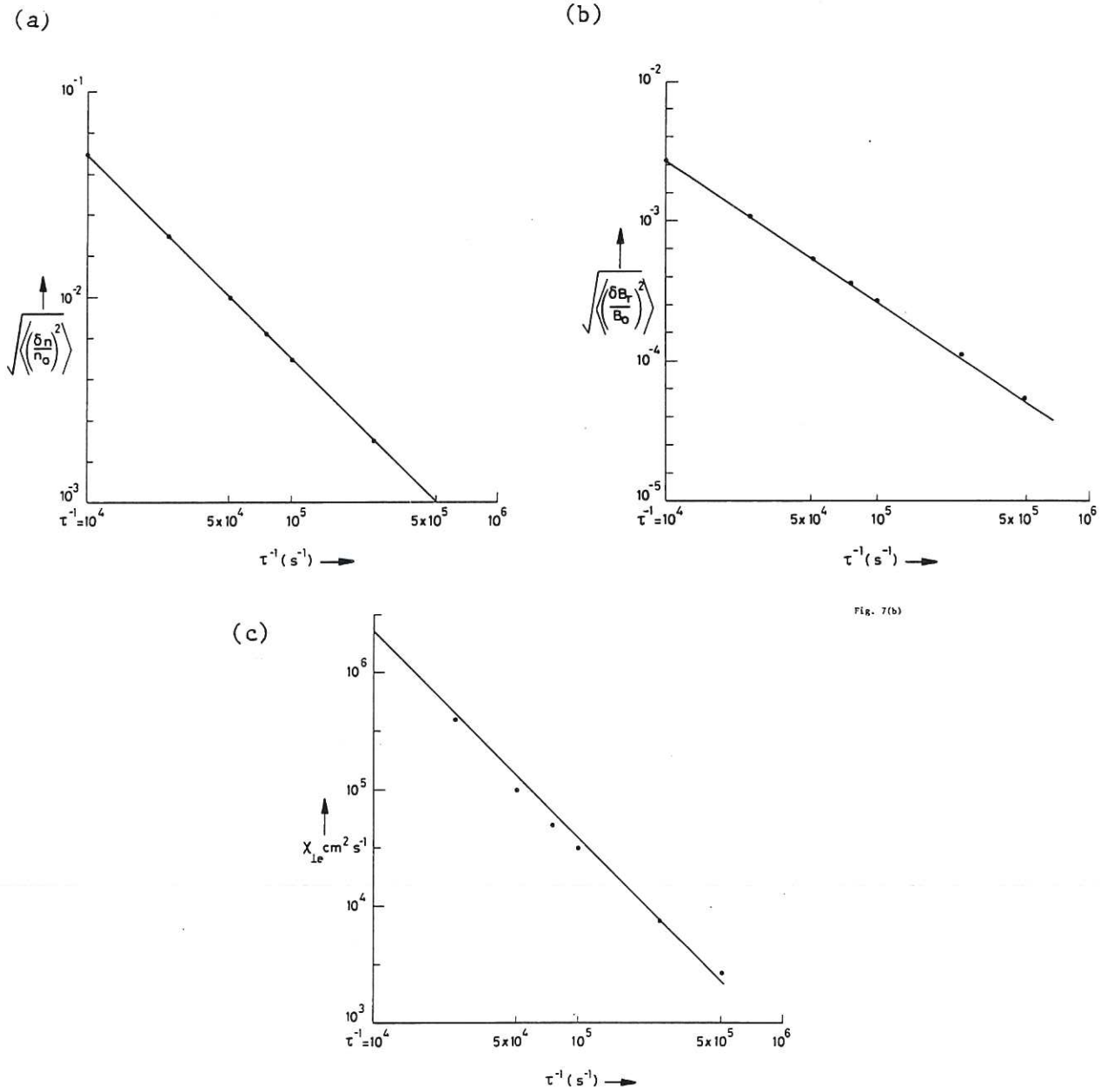

Fig. 7(b)

Fig. 7 Variation of turbulence properties with collision frequency (τ^{-1}). The quantities plotted are for TFR at $r/a=0.7$ with collision frequency $\tau^{-1}\propto n_0$, all other conditions being fixed (log-log plots).

(a) Assumed variation of RMS density fluctuation $\sqrt{(\delta n/n_0)^2}$ versus τ^{-1}.

(b) Calculated variation of RMS field fluctuation $\sqrt{(\delta B_r/B_0)^2}$ versus τ^{-1}.

(c) Calculated variation of thermal diffusivity ($\chi_{\perp e}$) versus τ^{-1}.

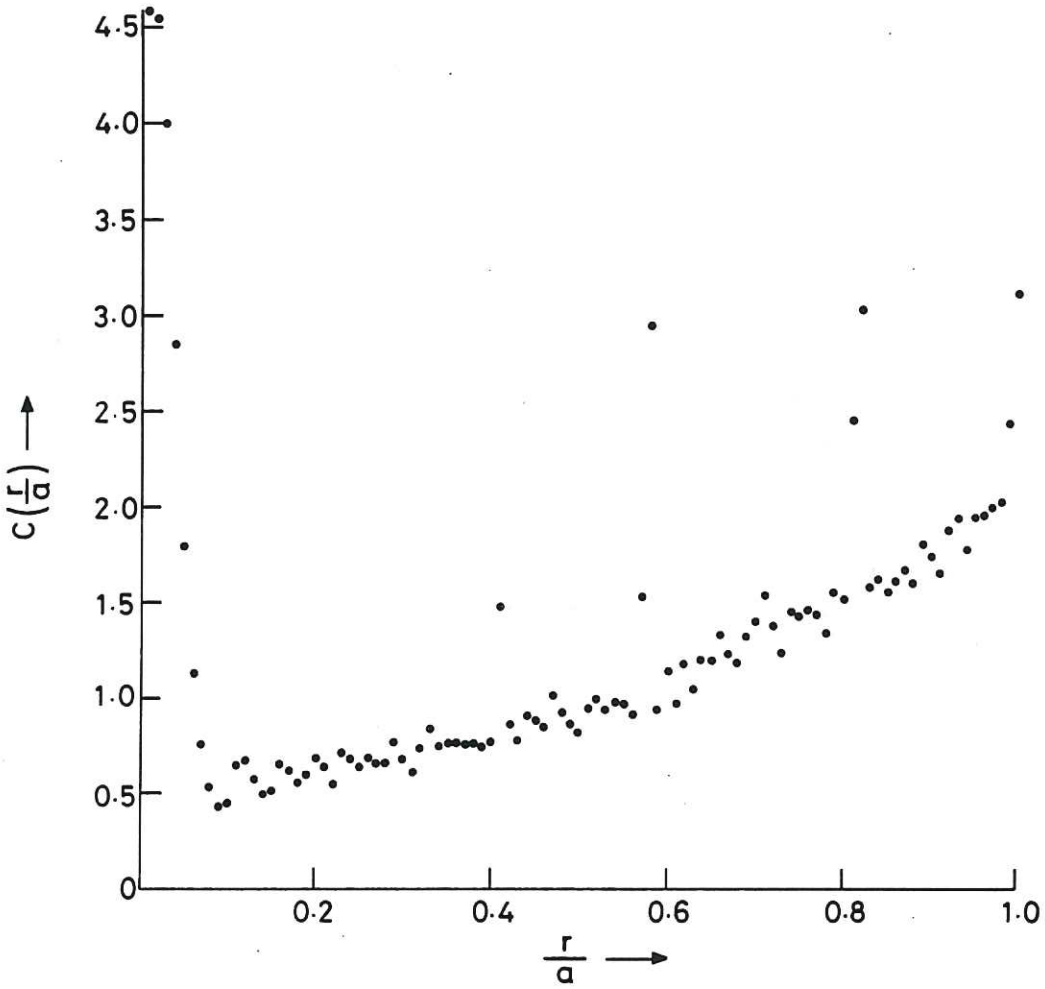

Fig. 8 Radial variation of the Knudsen correction factor $C(r/a) = \dfrac{\langle \chi_{\parallel_e} \rangle}{[(2\pi R)^2]/\tau}$, where $\langle \chi_{\parallel_e} \rangle$ is calculated from Eq.(31) and averaged over all the modes present for TFR conditions.